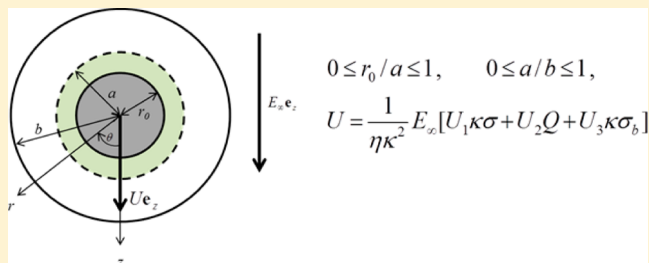


Electrophoresis of a Charged Soft Particle in a Charged Cavity with Arbitrary Double-Layer Thickness

Wei J. Chen and Huan J. Keh*

Department of Chemical Engineering, National Taiwan University, Taipei 10617, Taiwan, Republic of China

ABSTRACT: An analysis for the quasi-steady electrophoretic motion of a soft particle composed of a charged spherical rigid core and an adsorbed porous layer positioned at the center of a charged spherical cavity filled with an arbitrary electrolyte solution is presented. Within the porous layer, frictional segments with fixed charges are assumed to distribute uniformly. Through the use of the linearized Poisson–Boltzmann equation and the Laplace equation, the equilibrium double-layer potential distribution and its perturbation caused by the applied electric field are separately determined. The modified Stokes and Brinkman equations governing the fluid flow fields outside and inside the porous layer, respectively, are solved subsequently. An explicit formula for the electrokinetic migration velocity of the soft particle in terms of the fixed charge densities on the rigid core surface, in the porous layer, and on the cavity wall is obtained from a balance between its electrostatic and hydrodynamic forces. This formula is valid for arbitrary values of κa , λa , r_0/a , and a/b , where κ is the Debye screening parameter, λ is the reciprocal of the length characterizing the extent of flow penetration inside the porous layer, a is the radius of the soft particle, r_0 is the radius of the rigid core of the particle, and b is the radius of the cavity. In the limiting cases of $r_0 = a$ and $r_0 = 0$, the migration velocity for the charged soft sphere reduces to that for a charged impermeable sphere and that for a charged porous sphere, respectively, in the charged cavity. The effect of the surface charge at the cavity wall on the particle migration can be significant, and the particle may reverse the direction of its migration.



1. INTRODUCTION

A charged solid surface in contact with an electrolyte solution is adjacent to a diffuse cloud of ions carrying a total charge equal and opposite in sign to that of the solid surface. This distribution of fixed charges and adjoining diffuse ions is known as an electric double layer. When an external electric field is applied to a charged colloidal particle suspended in an electrolyte solution, a force is exerted on both parts of the double layer. The particle is attracted toward the electrode of its opposite sign, while the ambient counterions migrate in the other direction. This particle migration is termed “electrophoresis” and is a valuable tool for particle analysis and separation in a variety of physicochemical and biomedical systems. In the meantime, the fluid is dragged to flow by the motions of the particle and ions. To evaluate the transport properties such as the electrophoretic mobility of the particle, it is necessary to first solve for the electric potential distribution and velocity field in the electrolyte solution.

Assuming that the electric double layer is not distorted from its equilibrium state, Henry¹ derived an analytical formula for the electrophoretic mobility of a dielectric sphere of radius a with small zeta potential ζ for the entire range of κa , where κ^{-1} is the Debye length characterizing the thickness of the double layer. Later, O’Brien and White² took the double-layer distortion from equilibrium as a perturbation to obtain numerical solutions for the electrophoretic mobility of a dielectric sphere in an electrolyte solution which was applicable to arbitrary values of ζ and κa .

In real situations of electrophoresis, colloidal particles are seldom isolated and will move near solid boundaries. Electrophoresis in porous media is often applied because the unwanted mix-up caused by free convection due to Joule heating can be avoided. Microporous gels or membranes can be used to achieve high electric fields and permit separations based on both the size and the charge of the particles, such as DNA and RNA fragments, proteins, and other macromolecules.³ In capillary electrophoresis, gels in the column can minimize the particle diffusion, prevent the particle adsorption to the wall, and eliminate electroosmosis, while serving as the anticonvective media.⁴ Therefore, the boundary effects on electrophoresis of a colloidal sphere are of great importance and have been studied extensively for various cases of thin^{5–10} and thick^{11–14} electric double layers.

On the other hand, the surface of a colloidal particle is generally not hard. For example, surface layers are purposely formed by adsorbing long-chain polymers to make the suspended particles stable against flocculation.¹⁵ Even the surfaces of model colloids such as silica and polystyrene latex are “hairy” with a gel-like polymeric layer extending a substantial distance into the suspending medium from the bulk material inside the particle.¹⁶ In particular, the surface of a biological cell is not a hard wall, but rather is a permeable layer

Received: May 31, 2013

Revised: July 26, 2013

Published: July 30, 2013

ranging from protein molecules on the order of nanometers to cilia on the order of micrometers.¹⁷ Such particles can be modeled as a soft sphere having a central rigid core and an outer porous shell.^{18–23} Although general expressions were derived for the electrophoretic mobility of a soft sphere in an unbounded fluid,^{24–28} the boundary effects on the electrophoretic velocity of soft particles have rarely been analyzed.²⁹

The system of a spherical particle migrating at the center of a spherical cavity can be an idealized model for the electrophoresis in media constructed from connecting spherical pores.^{11–13} Also, the motion of each member of an array of hemispherically bichromal charged balls (about 100 μm in diameter) in its own elastomer-made and solvent-filled spherical cavity (which is only 10–40% larger than the ball) with either a monopole or a dipole on its wall between two thin, transparent plastic sheets controlled by imposing a voltage of either positive or negative polarity across the sheets has been applied to the technology of electric paper displays (known as Gyricon displays).^{30,31} In this article, the electrophoretic motion of a soft sphere composed of a charged rigid core and a charged porous layer in a concentric charged spherical cavity under a uniformly applied electric field is analyzed. The thicknesses of the porous layer and of the electric double layer are arbitrary relative to the radius of the particle. The linearized Poisson–Boltzmann equation and the modified Stokes/Brinkman equations are solved for the equilibrium double-layer potential distribution and the velocity field, respectively, for the fluid phase. The geometric symmetry in this model system allows an analytical solution of the electrokinetic migration velocity of the confined soft particle to be obtained in eqs 33 and 34.

2. ANALYSIS

We consider the quasi-steady electrophoretic motion of a charged soft sphere of radius a located at the center of a charged spherical cavity of radius b filled with an arbitrary electrolyte solution. As shown in Figure 1, the soft particle has a

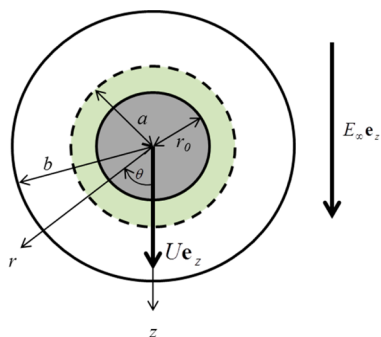


Figure 1. Geometric sketch for the electrophoresis of a charged soft sphere at the center of a charged spherical cavity.

charged rigid-sphere core of radius r_0 and an adsorbed surface layer of charged porous substance or polyelectrolytes of constant thickness $a - r_0$, where $0 \leq r_0/a \leq 1$. The porous surface layer is treated as a solvent-permeable and ion-impenetrable homogeneous shell in which fixed charges distribute uniformly. The thickness of the electric double layers around the particle and adjoining the cavity wall is arbitrary relative to the particle radius. The imposed electric field (external electric field in the absence of the particle) equals $E_\infty \mathbf{e}_z$, where E_∞ is a positive constant and \mathbf{e}_z is the unit vector in the z direction.

The origin of the spherical coordinate system (r, θ, ϕ) is taken at the particle center, and the polar axis $\theta = 0$ points toward the z direction. Obviously, the problem is axially symmetric about the z axis and independent of the coordinate ϕ .

To obtain the electrophoretic velocity of the soft particle within the cavity, we first need to determine the electric potential and fluid flow fields in the region between the rigid core of the particle and the cavity wall ($r_0 \leq r \leq b$).

2.1. Electric Potential Field. We follow previous analyses^{1,11,13,26} of electrophoresis to assume that the total electric potential distribution $\psi(r, \theta)$ in the electrolyte solution can be expressed as the sum of the equilibrium potential $\psi_1(r)$ that is induced by the fixed charges and diffuse ions in the electric double layers (spherically symmetric) and the perturbed potential $\psi_2(r, \theta)$ that arises from the applied electric field $E_\infty \mathbf{e}_z$:

$$\psi = \psi_1 + \psi_2 \quad (1)$$

which is valid if E_∞ is weak relative to the electric field associated with the double layers.

Through the use of the Debye–Hückel approximation, the equilibrium potential $\psi_1(r)$ is governed by the linearized Poisson–Boltzmann equation:

$$\nabla^2 \psi_1 = -\frac{1}{\epsilon} [\rho + h(r)Q] = \kappa^2 \psi_1 - h(r) \frac{Q}{\epsilon} \quad (2)$$

where ρ is the space charge density in the fluid phase, Q is the fixed charge density inside the porous surface layer of the soft particle, ϵ is the dielectric permittivity of the electrolyte solution, and $h(r)$ is a unit step function which equals unity if $r_0 < r < a$ (inside the porous surface layer) and zero if $a < r < b$ (outside the soft particle). In eq 2, Q , ϵ , and κ are taken as constants.

The boundary conditions for ψ_1 are

$$r = r_0:$$

$$\frac{d\psi_1}{dr} = -\frac{\sigma}{\epsilon} \quad (3)$$

$$r = a:$$

$$\psi_1 \text{ and } \epsilon \frac{d\psi_1}{dr} \text{ are continuous} \quad (4)$$

$$r = b:$$

$$\frac{d\psi_1}{dr} = \frac{\sigma_b}{\epsilon} \quad (5)$$

where σ and σ_b are the uniform surface charge densities of the rigid core of the soft particle and the cavity wall, respectively. Equations 3 and 5 state that the Gauss condition holds at the dielectric core surface and cavity wall, where the core and cavity phases have no free charges in their interiors or their dielectric constants are much less than that of the electrolyte solution.

Experimental data for the porous surface layers of human erythrocytes,³² rat lymphocytes,³³ and poly(*N*-isopropylacrylamide) hydrogels³⁴ in electrolyte solutions indicate that the magnitude of the fixed charge density Q can be as high as $8.7 \times 10^6 \text{ C/m}^3$. For the surface charge density σ or σ_b , an experimental study on the AgI surface in contact with aqueous solutions reported that its value changes from 0 to -0.035 C/m^2 upon increasing the pAg from 5.6 to 11.³⁵

The solution to eqs 2–5 is obtained as

$$\psi_1 = \frac{1}{\epsilon\kappa^2} [\psi_{11}(r)\kappa\sigma + \psi_{12}(r)Q + \psi_{13}(r)\kappa\sigma_b] \quad (6)$$

where

$$\psi_{11}(r) = \frac{2(\kappa r_0)^2 e^{\kappa(b+r_0)}}{A\kappa r} \{ \kappa b \cosh[\kappa(b-r)] - \sinh[\kappa(b-r)] \} \quad (7)$$

$$\psi_{12}(r) = \frac{e^{-\kappa r}}{2A\kappa r} \{ [e^{\kappa a}(\kappa a - 1)(\kappa r_0 + 1) - e^{\kappa(2r_0-a)}(\kappa a + 1)(\kappa r_0 - 1)] [e^{2\kappa b}(\kappa b - 1) + e^{2\kappa r}(\kappa b + 1)] \} \quad (8a)$$

for $a < r < b$

$$\psi_{12}(r) = \frac{e^{\kappa(2b-a+2r_0-r)}}{2A\kappa r} \left\{ \frac{1}{A} + e^{\kappa(a-2b)}(\kappa b + 1)(\kappa r_0 - 1) [e^{\kappa a}(\kappa a - 1) - 2e^{\kappa r}\kappa r] - e^{\kappa(r-2r_0)}(\kappa b - 1)(\kappa r_0 + 1) [e^{\kappa r}(\kappa a + 1) - 2e^{\kappa a}\kappa r] + e^{2\kappa(a-b-r_0+r)}(\kappa a - 1)(\kappa b + 1)(\kappa r_0 + 1) + \kappa[b - r_0(\kappa b - 1) - a(\kappa b - 1)(\kappa r_0 - 1)] \right\} \quad \text{for } r_0 < r < a \quad (8b)$$

$$\psi_{13}(r) = \frac{2(\kappa b)^2 e^{\kappa(b+r_0)}}{A\kappa r} \{ \kappa r_0 \cosh[\kappa(r-r_0)] + \sinh[\kappa(r-r_0)] \} \quad (9)$$

and

$$A = e^{2\kappa b}(\kappa b - 1)(\kappa r_0 + 1) - e^{2\kappa r_0}(\kappa b + 1)(\kappa r_0 - 1) \quad (10)$$

The electric potential $\psi_2(r, \theta)$ caused by the applied electric field $E_\infty \mathbf{e}_z$ is governed by the Laplace equation

$$\nabla^2 \psi_2 = 0 \quad (11)$$

This potential field is the zeroth-order perturbation in the fixed charge densities σ , Q , and σ_b , which together with the potential field ψ_1 , zeroth-order perturbation in the applied electric field, will be sufficient to determine the particle velocity correct to the first orders in E_∞ , σ , Q , and σ_b .

The boundary condition for ψ_2 at the nonconductive surface of the rigid core of the soft particle is

$$r = r_0:$$

$$\frac{\partial \psi_2}{\partial r} = 0 \quad (12)$$

Given the applied electric field $E_\infty \mathbf{e}_z$, a legitimate boundary condition for ψ_2 at the cavity wall is

$$r = b:$$

$$\psi_2 = -E_\infty r \cos \theta \quad (13)$$

in the Dirichlet approach^{13,36–38} or

$$r = b:$$

$$\frac{\partial \psi_2}{\partial r} = -E_\infty \cos \theta \quad (14)$$

in the Neumann approach.^{11,26,39,40} Both approaches give rise to the uniformly applied electric field in the fluid phase when

the particle does not exist. In eq 13, we have set $\psi_2 = 0$ on the plane $z = 0$ without loss in generality. In eq 14, the tangential component of the potential gradient at the cavity wall is not specified.

The solution to eq 11 subject to the boundary conditions in eqs 12 and 13 or 14 is

$$\psi_2 = -\frac{E_\infty}{\nu} \left(r + \frac{r_0^3}{2r^2} \right) \cos \theta \quad (15)$$

where $\nu = 1 + (r_0/b)^3/2$ if the Dirichlet condition in eq 13 is employed, whereas $\nu = 1 - (r_0/b)^3$ if the Neumann condition in eq 14 is used. In the limit $r_0/b \rightarrow 0$, as expected, eqs 13 and 14 become identical (with $\nu = 1$) and eq 15 reduces to the potential distribution for a porous sphere ($r_0 = 0$) in a cavity of radius b (uniform potential gradient) or a nonconductive rigid sphere of radius r_0 in an unbounded medium ($b \rightarrow \infty$).

2.2. Fluid Flow Field. The fluid motions outside and inside the porous surface layer of the soft particle are governed by the Stokes and Brinkman equations, respectively, modified with an additional electric force term. Thus, we can write

$$\eta \nabla^2 \mathbf{v} - h(r)f\mathbf{v} = \nabla p + \rho \nabla \psi \quad (16)$$

$$\nabla \cdot \mathbf{v} = 0 \quad (17)$$

where $\mathbf{v}(r, \theta)$ and $p(r, \theta)$ are the fluid velocity and dynamic pressure, respectively, η is the fluid viscosity, and f is the friction coefficient within the porous surface layer per unit volume of the fluid; η and f are assumed to be constant.

Because the reference frame is taken to travel with the particle, the boundary conditions for the fluid velocity are

$$r = r_0:$$

$$\mathbf{v} = \mathbf{0} \quad (18)$$

$$r = a:$$

$$\mathbf{v} \text{ and } \mathbf{e}_r \cdot \boldsymbol{\sigma} \text{ are continuous} \quad (19)$$

$$r = b:$$

$$\mathbf{v} \rightarrow -U\mathbf{e}_z \quad (20)$$

where $\boldsymbol{\sigma} = -p\mathbf{I} + \eta[\nabla \mathbf{v} + (\nabla \mathbf{v})^T]$ is the hydrodynamic stress tensor, in which \mathbf{I} is the unit dyadic, \mathbf{e}_r is the unit normal vector outward from the particle surface, and U is the electrokinetic migration velocity of the soft sphere to be determined.

Using eqs 1 and 2, one can express eq 16 as

$$\nabla^2 \mathbf{v} - h(r)\lambda^2 \mathbf{v} = \frac{1}{\eta} (\nabla p - \epsilon \kappa^2 \psi_1 \nabla \psi_2) \quad (21)$$

to the first orders of the fixed charge densities σ , Q , and σ_b , where $\lambda = (f/\eta)^{1/2}$. The reciprocal of the parameter λ is the Brinkman screening (shielding) length characterizing the extent of flow penetration inside the porous surface layer. For some model porous particles made of steel wool (in glycerin–water solution)⁴¹ and plastic foam slab (in silicon oil),⁴² experimental values of $1/\lambda$ can be as high as 0.4 mm, whereas in the surface regions of human erythrocytes,³² rat lymphocytes,³³ and grafted polymer microcapsules⁴³ in salt solutions, values of $1/\lambda$ were found to be about 3 nm. Note that $1/\lambda^2$ is the “permeability” of the porous medium in the Brinkman equation, which is related to its pore size and porosity.

The solutions for the r and θ components of \mathbf{v} and p subject to eqs 6, 15, and 17–21 are

$$v_r = \frac{1}{\eta\kappa^2} E_\infty [\nu_{r1}(r)\kappa\sigma + \nu_{r2}(r)Q + \nu_{r3}(r)\kappa\sigma_b] \cos \theta \quad (22)$$

$$v_\theta = -\frac{\tan \theta}{2r} \frac{d}{dr}(r^2 v_r) \quad (23)$$

$$p = \frac{E_\infty}{\kappa^2 a} [p_1(r)\kappa\sigma + p_2(r)Q + p_3(r)\kappa\sigma_b] \cos \theta \quad (24)$$

where

$$\begin{aligned} v_{ri}(r) = & C_{1i} + C_{2i} \frac{a}{r} + C_{3i} \left(\frac{a}{r}\right)^3 + C_{4i} \left(\frac{r}{a}\right)^2 + \frac{1}{5} \left(\frac{r}{a}\right)^2 J_{0i}(r) \\ & - J_{2i}(r) + \frac{a}{r} J_{3i}(r) - \frac{1}{5} \left(\frac{a}{r}\right)^3 J_{5i}(r) \quad \text{for } a < r < b \end{aligned} \quad (25a)$$

$$\begin{aligned} v_{ri}(r) = & C_{5i} + C_{6i} \left(\frac{a}{r}\right)^3 + C_{7i} \left(\frac{a}{r}\right)^3 \alpha(\lambda r) + C_{8i} \left(\frac{a}{r}\right)^3 \beta(\lambda r) \\ & - \frac{2}{(\lambda a)^2} \left[J_{0i}(r) - \left(\frac{a}{r}\right)^3 J_{3i}(r) + \frac{3\alpha(\lambda r)}{(\lambda r)^3} J_{\beta i}(r) \right. \\ & \left. - \frac{3\beta(\lambda r)}{(\lambda r)^3} J_{\alpha i}(r) \right] \quad \text{for } r_0 < r < a \end{aligned} \quad (25b)$$

$$\begin{aligned} p_i(r) = & C_{2i} \left(\frac{a}{r}\right)^2 + 10C_{4i} \frac{r}{a} + \left(\frac{a}{r}\right)^2 J_{3i}(r) + 2\frac{r}{a} J_{0i}(r) \\ & - \frac{1}{\nu a} \left(r + \frac{r_0^3}{2r^2} \right) \psi_{1i}(r) \quad \text{for } a < r < b \end{aligned} \quad (26a)$$

$$\begin{aligned} p_i(r) = & \lambda^2 a r \left[\frac{C_{6i}}{2} \left(\frac{a}{r}\right)^3 - C_{5i} \right] + 2\frac{r}{a} J_{0i}(r) + \left(\frac{a}{r}\right)^2 J_{3i}(r) \\ & - \frac{1}{\nu a} \left(r + \frac{r_0^3}{2r^2} \right) \psi_{1i}(r) \quad \text{for } r_0 < r < a \end{aligned} \quad (26b)$$

$$\alpha(x) = x \cosh x - \sinh x \quad (27a)$$

$$\beta(x) = x \sinh x - \cosh x \quad (27b)$$

$$J_{ni}(r) = \frac{(\kappa a)^2}{6\nu} \int_a^r \left(\frac{r}{a}\right)^n \left[2 + \left(\frac{r_0}{r}\right)^3 \right] \frac{d\psi_{1i}}{dr} dr \quad (28a)$$

$$J_{\alpha i}(r) = \frac{(\kappa a)^2}{6\nu} \int_a^r \alpha(\lambda r) \left[2 + \left(\frac{r_0}{r}\right)^3 \right] \frac{d\psi_{1i}}{dr} dr \quad (28b)$$

$$J_{\beta i}(r) = \frac{(\kappa a)^2}{6\nu} \int_a^r \beta(\lambda r) \left[2 + \left(\frac{r_0}{r}\right)^3 \right] \frac{d\psi_{1i}}{dr} dr \quad (28c)$$

$i = 1, 2$, and 3 , and the expressions for the dimensionless coefficients C_{ni} are lengthy and given in ref 44.

2.3. Particle Velocity. The total force acting on the charged particle undergoing electrophoretic migration in an electrolyte solution can be expressed as the sum of the electrostatic and hydrodynamic forces. The electrostatic force is given by

$$\mathbf{F}_e = \int_{r=a} \boldsymbol{\sigma}^E \cdot \mathbf{e}_r dS \quad (29)$$

where the Maxwell stress

$$\boldsymbol{\sigma}^E = \varepsilon \left(\mathbf{E}\mathbf{E} - \frac{1}{2} |\mathbf{E}|^2 \mathbf{I} \right) \quad (30)$$

and $\mathbf{E} = -\nabla\psi$ is the electric field. Substituting eq 30 into eq 29 and using the fact that the net electrostatic force acting on the particle at the equilibrium state is zero, one obtains

$$\mathbf{F}_e = 2\pi a^2 \varepsilon \int_0^\pi \nabla\psi_1 \nabla\psi_2 \cdot \mathbf{e}_r \sin \theta d\theta \quad (31)$$

correct to the first order in σ , Q , σ_b , and E_∞ . The hydrodynamic force exerted on the soft sphere is given by the integral of the hydrodynamic stress over the particle surface:

$$\mathbf{F}_h = 2\pi a^2 \int_0^\pi \{ -p\mathbf{e}_r + \eta[\nabla\mathbf{v} + (\nabla\mathbf{v})^T] \cdot \mathbf{e}_r \} \sin \theta d\theta \quad (32)$$

At the quasi-steady state, the net force exerted on the particle must be zero. Applying this constraint to the sum of eqs 31 and 32 with the substitution of eqs 6, 15, and 22–24, we obtain the electrokinetic migration velocity of the confined soft sphere as

$$U = \frac{1}{\eta\kappa^2} E_\infty [U_1\kappa\sigma + U_2Q + U_3\kappa\sigma_b] \quad (33)$$

where

$$\begin{aligned} U_i = & \frac{1}{B_2} \left\{ \frac{B_0}{\nu(\kappa a)^2} \left[\frac{\kappa^2}{6a} (2a^3 + r_0^3) \psi_{1i}(a) + a \frac{d\psi_{1i}}{dr}(a) \right] \right. \\ & + B_1 J_{0i}(b) + B_2 J_{2i}(b) + B_3 J_{3i}(b) + B_4 J_{5i}(b) \\ & \left. + B_5 J_{0i}(r_0) + B_6 J_{3i}(r_0) + B_7 J_{\alpha i}(r_0) + B_8 J_{\beta i}(r_0) \right\} \end{aligned} \quad (34)$$

and the dimensionless coefficients B_n are given in ref 44.

Note that U_1 , U_2 , and U_3 can be taken as the dimensionless electrophoretic mobility of a soft sphere with a charged rigid core and an uncharged porous surface layer ($Q = 0$) in an uncharged cavity ($\sigma_b = 0$), the electrophoretic mobility of a soft sphere with an uncharged rigid core ($\sigma = 0$) and a charged surface layer in an uncharged cavity, and the electrokinetic mobility of an uncharged soft sphere ($\sigma = Q = 0$) in a charged cavity, respectively. These dimensionless mobilities are functions of the electrokinetic radius κa , the shielding parameter λa , and the radius ratio r_0/a of the particle as well as the particle-to-cavity radius ratio a/b . Due to the linearity of the problem, the effects of the fixed charges of the particle and cavity on the particle migration can be superimposed directly. The charge on the cavity wall alters the motion of the particle through the electroosmotic recirculation flow developing from the interaction of the imposed electric field with the electric double layer adjacent to the charged wall (dominant at large κa) and the charged-wall-induced electric potential over the porous layer and core surface of the soft particle.

3. RESULTS AND DISCUSSION

The electrokinetic migration velocity of a charged soft sphere situated at the center of a charged spherical cavity under the imposed electric field E_∞ is obtained in eq 33. In this section, we first consider this velocity for the two particular cases of the soft sphere: an impermeable sphere (section 3.1) and a porous sphere (section 3.2). Results for the general case of a soft sphere will then be presented in section 3.3.

3.1. Electrokinetic Migration of a Rigid Sphere in a Cavity. When there is no permeable layer on the surface of the rigid core of a soft sphere undergoing electrophoresis in a concentric spherical cavity, the particle reduces to an impermeable sphere of radius $a = r_0$, the term $U_2 Q$ in eq 33 is trivial, and the dimensionless mobility parameters U_1 and U_3 calculated from eq 34 are functions of the electrokinetic particle radius κa and the particle-to-cavity radius ratio a/b only. The cavity-to-particle surface charge density ratio σ_b/σ corresponds to the strength and direction of the effect resulting from the cavity-induced electroosmotic flow and particle surface potential relative to the electrophoretic driving force exerted on the particle.

In the limit of thin electric double layers ($\kappa a \rightarrow \infty$) for a rigid sphere in a spherical cavity, eq 34 becomes

$$U_1 = \frac{(1 - \xi)^2}{(1 - \xi^5)\nu} \left(1 + 2\xi + 3\xi^2 + \frac{3}{2}\xi^3 \right) \quad (35a)$$

$$U_3 = \frac{(1 - \xi)^2}{(1 - \xi^5)\nu} \left(1 + 2\xi + \frac{4}{3}\xi^2 + \frac{7}{6}\xi^3 + \xi^4 + \frac{2}{3}\xi^5 + \frac{1}{3}\xi^6 \right) \quad (35b)$$

where $\xi = a/b$ and ν has been defined right after eq 15. Note that eq 33 together with eqs 35a and 35b predicts a vanishing particle velocity in this limit with constant surface charge densities. In the limit of thick double layers ($\kappa a \rightarrow 0$), eq 34 results in

$$U_1 = \frac{\kappa a(2 + \xi^3)(1 - \xi)^2(4 + 7\xi + 4\xi^2)}{12(1 + \xi + \xi^2)(1 + \xi + \xi^2 + \xi^3 + \xi^4)\nu} \quad (36a)$$

$$U_3 = \frac{\kappa a\xi^3(1 - \xi)^2(4 + 7\xi + 4\xi^2)}{4(1 + \xi + \xi^2)(1 + \xi + \xi^2 + \xi^3 + \xi^4)\nu} \quad (36b)$$

which still leads to a finite particle velocity according to eq 33.

In the limit $a/b = 0$ (the cavity wall is at an infinite distance from the particle and $\nu = 1$), eq 34 reduces to

$$U_1 = \frac{\kappa a}{\kappa a + 1} \{ 1 - e^{\kappa a} [5E_7(\kappa a) - 2E_5(\kappa a)] \} \quad (37a)$$

$$U_3 = 1 \quad (37b)$$

and

$$E_n(x) = \int_1^\infty t^{-n} e^{-xt} dt \quad (38)$$

In the limit $a/b = 1$ (the particle fills up the cavity completely), eq 34 leads to $U_1 = U_3 = 0$ for all cases except that, when $\kappa a \rightarrow \infty$, $U_1 = U_3 = 1/2$ (but eq 33 still predicts a zero particle velocity in this limit) if the Neumann boundary condition in eq 14 is used for the applied electric potential ψ_2 at the cavity wall. It can be shown that eqs 35a–37b are consistent with the results obtained for the electrokinetic migration of a rigid sphere in a concentric spherical cavity with constant surface (ζ) potentials.^{11,13}

The mobility parameters U_1 and U_3 for a rigid sphere in a spherical cavity, as calculated from eq 34, are plotted versus the relevant parameters in Figures 2 and 3, respectively. For specified values of κa and a/b , the values of U_1 and U_3 are always positive and those predicted from using the Neumann boundary condition in eq 14 for the applied electric potential at

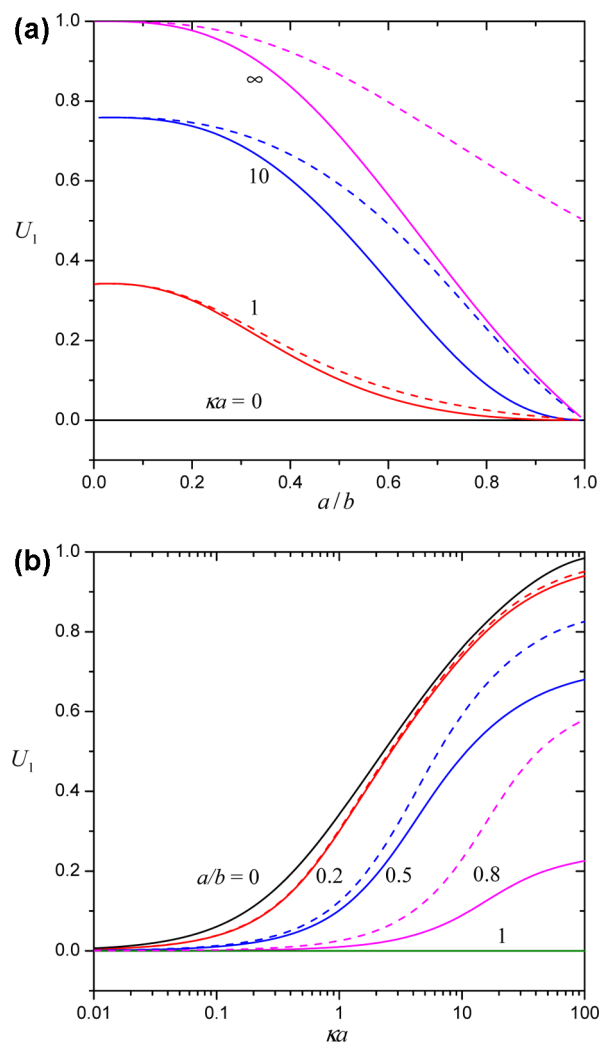


Figure 2. Plots of the mobility parameter U_1 for a charged rigid sphere in a spherical cavity as calculated from eq 34 versus the parameters κa and a/b . The solid and dashed curves represent the cases using the Dirichlet boundary condition in eq 13 and the Neumann condition in eq 14, respectively.

the cavity wall are always greater than their corresponding results obtained from using the Dirichlet boundary condition in eq 13. For a given finite value of κa , U_1 and U_3 are decreasing functions of a/b and vanish at $a/b = 1$. When $\kappa a \rightarrow \infty$, as predicted by eqs 35a and 35b, U_1 and U_3 decrease with an increase in a/b from unity at $a/b = 0$ to zero (if the Dirichlet condition is adopted) or to 1/2 (if the Neumann condition is used) at $a/b = 1$. This difference in the results of these mobility parameters in this limit between the two different boundary conditions suggests that the Dirichlet condition might be a more reasonable choice than the Neumann condition for the applied electric potential at the cavity wall. For a fixed value of a/b , U_1 and U_3 increase monotonically with an increase in κa (a decrease in the electric-double-layer overlap) from zero at $\kappa a = 0$. The differences in the results of these mobility parameters between the Dirichlet and Neumann boundary conditions are greater for a larger value of κa (a relatively thinner double layer) or a/b (except as $a/b \rightarrow 1$).

To use eq 33 to determine the electrokinetic migration velocity of a charged rigid sphere in a charged cavity, not only the parameters κa and a/b but also the surface charge densities

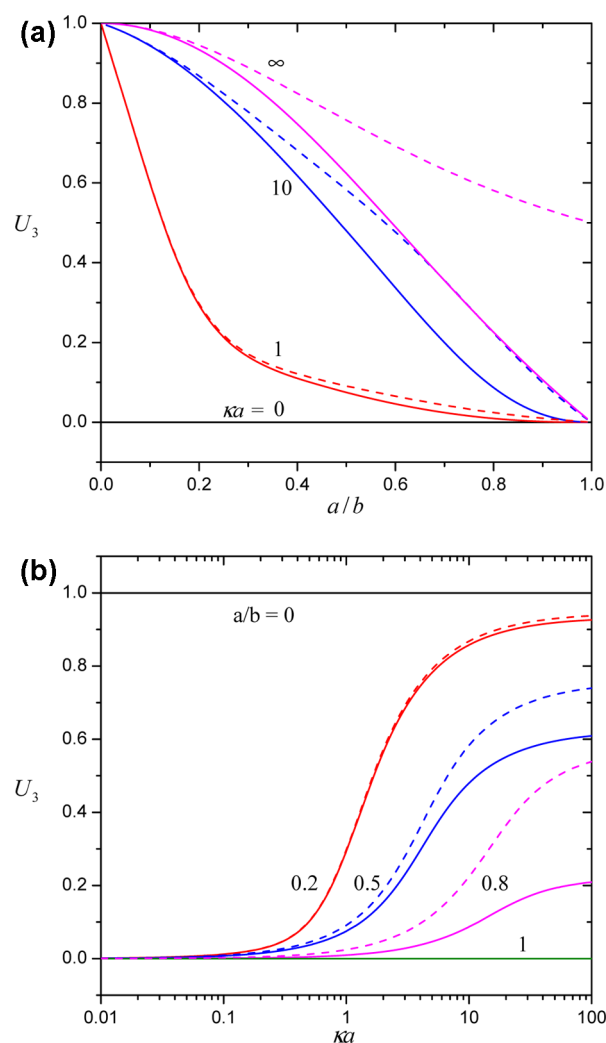


Figure 3. Plots of the mobility parameter U_3 for a rigid sphere in a charged spherical cavity as calculated from eq 34 versus the parameters κa and a/b . The solid and dashed curves represent the cases using the Dirichlet boundary condition in eq 13 and the Neumann condition in eq 14, respectively.

σ and σ_b have to be specified. Figures 2 and 3 show that the values of U_1 and U_3 are of the same sign and order of magnitude. Thus, for the case of a charged rigid sphere undergoing electrophoresis in a charged cavity with surface charge densities of the same/opposite signs, the effect of the cavity wall will enhance/reduce the electrophoretic velocity of the particle. This tendency can be seen clearly in Figure 4, in which the normalized particle velocity $\eta\kappa U/\sigma E_\infty$ ($=U_1 + U_3\sigma_b/\sigma$) is plotted versus the cavity-to-particle surface charge density ratio σ_b/σ (as a linear function) for various values of κa and a/b . As expected, the effect of the surface charge at the cavity wall on the migration of the particle can be significant as the magnitude of σ_b/σ is large. When the value of σ_b/σ is smaller than about -1 , the particle may reverse the direction of its velocity from that of electrophoresis in an unbounded fluid. Again, the magnitude of $\eta\kappa U/\sigma E_\infty$ predicted from using the Neumann boundary condition for the applied electric potential at the cavity wall is greater than that from using the Dirichlet boundary condition, and this magnitude in general increases with an increase in κa and decreases with an increase in a/b .

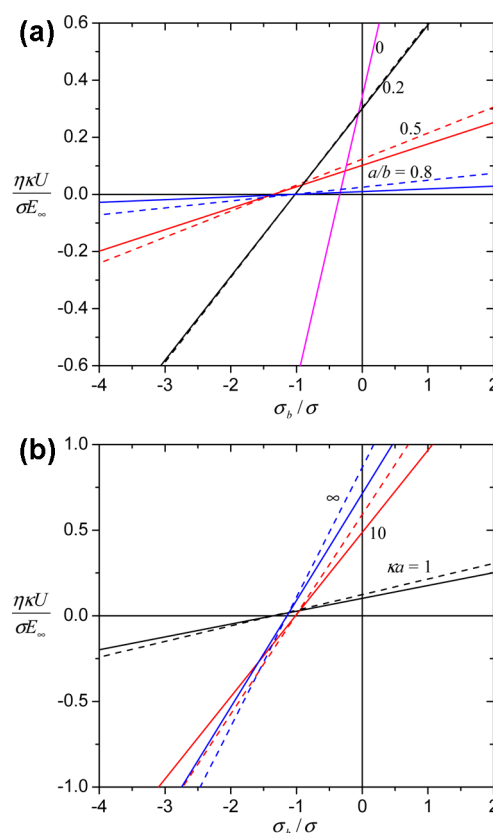


Figure 4. Plots of the normalized electrokinetic migration velocity $\eta\kappa U/\sigma E_\infty$ for a charged rigid sphere in a charged spherical cavity as calculated from eq 33 versus the surface charge density ratio σ_b/σ : (a) $\kappa a = 1$; (b) $a/b = 0.5$. The solid and dashed lines denote the cases using the Dirichlet boundary condition in eq 13 and the Neumann condition in eq 14, respectively.

If the particle moves away from the center of a cavity with a like/oppositely charged wall, it will experience a stronger repulsive/attractive force on the part of the particle surface close to the cavity wall than on that far from the wall with a reduction/enhancement in the particle velocity. In fact, an eccentrically positioned particle in a cavity can move due to this electrostatic interaction, even in the absence of the external field.

3.2. Electrokinetic Migration of a Porous Sphere in a Cavity. When the rigid core of a soft sphere undergoing electrophoresis in a concentric spherical cavity disappears ($r_0 = 0$), the particle becomes a permeable sphere (such as polymer coils or colloidal flocs) of radius a , the term $U_1\kappa\sigma$ in eq 33 is trivial, and the mobility parameters U_2 and U_3 calculated from eq 34 are functions of the electrokinetic radius κa , the shielding parameter λa , and the radius ratio a/b and are independent of the boundary condition for ψ_2 at the cavity wall given by eq 13 or 14 ($\nu = 1$). The dimensionless cavity-to-particle fixed charge density ratio $\kappa\sigma_b/Q$ corresponds to the strength and direction of the effect resulting from the cavity-induced electroosmotic flow and potential distribution relative to the electrophoretic driving force acting on the particle. When $\lambda a \rightarrow \infty$, the resistance to the fluid motion is infinitely large and the relative fluid velocity vanishes inside the porous particle. When $\lambda a = 0$, the porous particle does not exert resistance to the fluid motion.

In the limit of thin electric double layers ($\kappa a \rightarrow \infty$) for a porous sphere in a spherical cavity, eq 34 becomes

$$U_2 = \left(\frac{\kappa}{\lambda}\right)^2 \quad (39a)$$

$$U_3 = \left\{ \lambda a \left[10\xi^2(1 - \xi^3) - \frac{1}{3}(\lambda a)^2(3 - 5\xi^2 + 2\xi^5) \right] \right. \\ \left. \cosh \lambda a - [10\xi^2(1 - \xi^3) - (\lambda a)^2(1 - 5\xi^2 + 4\xi^5)] \right. \\ \left. \sinh \lambda a \right\} \left\{ \lambda a [15\xi^5 - (\lambda a)^2(1 - \xi^5)] \cosh \lambda a \right. \\ \left. - [15\xi^5 - (\lambda a)^2(1 - 6\xi^5)] \sinh \lambda a \right\}^{-1} \quad (39b)$$

In the limit of thick double layers ($\kappa a \rightarrow 0$), eq 34 leads to

$$U_2 = \frac{(\kappa a)^2}{18} \{ \lambda a [270\xi^5 - 6(\lambda a)^2(1 + 10\xi^3 - 21\xi^5 \\ + 10\xi^6) - (\lambda a)^4(1 - \xi)^4(4 + 7\xi + 4\xi^2)] \\ \cosh \lambda a - 3[90\xi^5 - 2(\lambda a)^2(1 + 10\xi^3 - 36\xi^5 \\ + 10\xi^6) + (\lambda a)^4\xi(1 - \xi)^3(3 + 9\xi + 8\xi^2)] \sinh \lambda a \} \\ \{ (\lambda a)^3[15\xi^5 - (\lambda a)^2(1 - \xi^5)] \\ \cosh \lambda a - (\lambda a)^2[15\xi^5 - (\lambda a)^2(1 - 6\xi^5)] \\ \sinh \lambda a \}^{-1} \quad (40a)$$

$$U_3 = \frac{(\kappa a)^3}{420} \{ \lambda a [-420\xi^4(2 - 5\xi^3 + 3\xi^5) + 5(\lambda a)^2\xi^2 \\ (12 - 28\xi^2 - 21\xi^3 + 70\xi^5 - 33\xi^7) \\ - (\lambda a)^4(1 - \xi)^4(1 + \xi)(3 + 9\xi + 11\xi^2 + 9\xi^3 \\ + 3\xi^4)] \cosh \lambda a + [420\xi^4(2 - 5\xi^3 + 3\xi^5) \\ + (\lambda a)^4(3 - 30\xi^2 + 35\xi^4 + 42\xi^5 - 80\xi^7 + 30\xi^9) \\ - 15(\lambda a)^2\xi^2(4 - 28\xi^2 - 7\xi^3 + 70\xi^5 - 39\xi^7)] \\ \sinh \lambda a \} \{ (\lambda a)^3\xi^3[15\xi^5 - (\lambda a)^2(1 - \xi^5)] \\ \cosh \lambda a - (\lambda a)^2\xi^3[15\xi^5 - (\lambda a)^2(1 - 6\xi^5)] \\ \sinh \lambda a \}^{-1} \quad (40b)$$

In the limit $a/b = 0$ (the cavity wall is at an infinite distance from the particle), eq 34 reduces to

$$U_2 = \left(\frac{\kappa}{\lambda}\right)^2 + \frac{1}{3} \left(1 + e^{-2\kappa a} - \frac{1 - e^{-2\kappa a}}{\kappa a} \right) \\ + \frac{1}{3} \left(\frac{\kappa^2}{\lambda^2 - \kappa^2} \right) \left(1 + \frac{1}{\kappa a} \right) \\ \left[\left(\frac{\lambda}{\kappa} \right)^2 \frac{\kappa a (1 + e^{-2\kappa a}) - 1 + e^{-2\kappa a}}{\lambda a \coth(\lambda a) - 1} - 1 + e^{-2\kappa a} \right] \quad (41a)$$

$$U_3 = 1 \quad (41b)$$

Equation 41a is the same as the corresponding formula obtained for a charged porous sphere in an unbounded electrolyte solution.^{45–47} In the limit $a/b = 1$ (the particle fills up the cavity completely), eq 34 gives $U_2 = (\kappa/\lambda)^2$ (in contrast

to $U_1 = 0$ for the case of a charged rigid sphere considered in section 3.1) and $U_3 = 0$.

In Figures 5 and 6, the mobility parameters U_2 and U_3 for a porous sphere in a spherical cavity calculated from eq 34 are

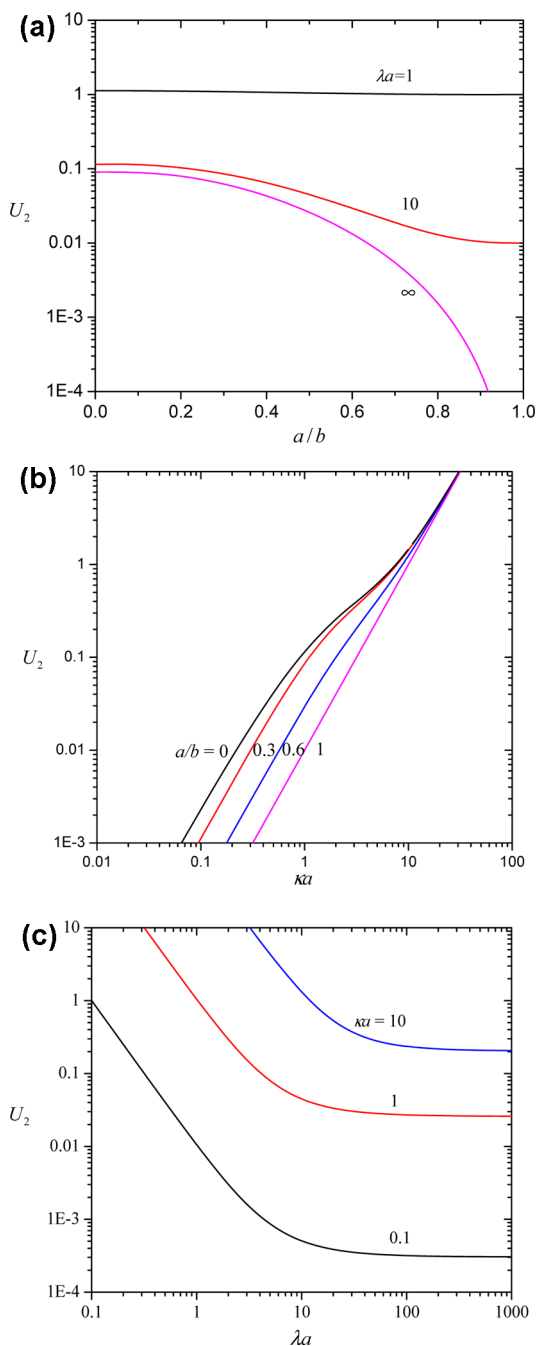


Figure 5. Plots of the mobility parameter U_2 for a charged porous sphere in a spherical cavity as calculated from eq 34: (a) $\kappa a = 1$; (b) $\lambda a = 10$; (c) $a/b = 0.5$.

plotted as functions of the parameters κa , λa , and a/b . Analogous to the case of a confined rigid sphere, U_2 and U_3 are always positive and of the same order of magnitude. For given values of λa and a/b , U_2 and U_3 increase monotonically with an increase in κa from zero at $\kappa a = 0$ and are proportional to $(\kappa a)^2$ and $(\kappa a)^3$, respectively, in wide ranges. For fixed values of κa and a/b , U_2 and U_3 decrease monotonically with an increase in λa (the relative resistance for the fluid flow inside the particle);

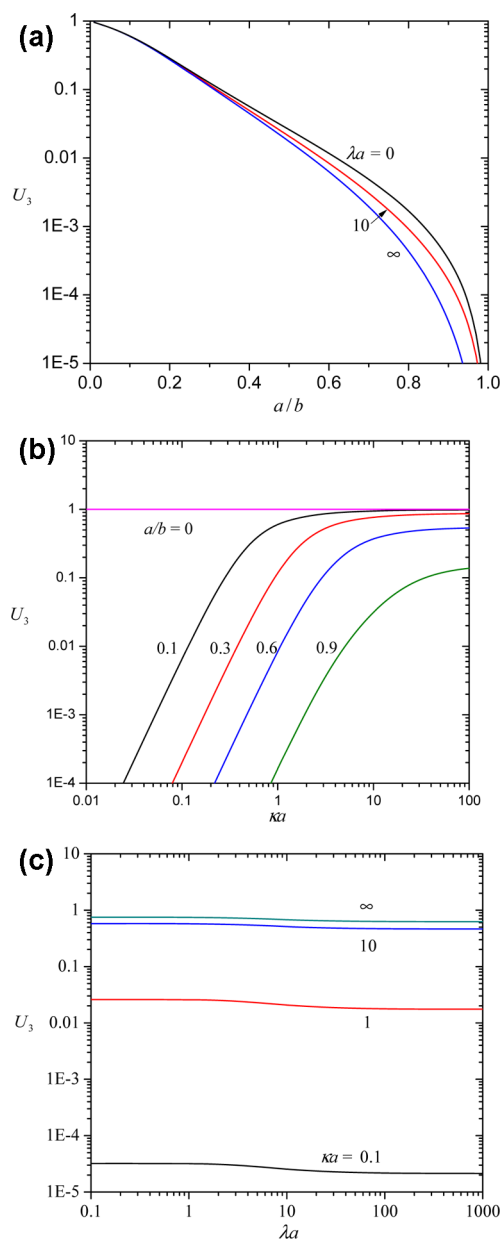


Figure 6. Plots of the mobility parameter U_3 for a porous sphere in a charged spherical cavity as calculated from eq 34: (a) $\kappa a = 1$; (b) $\lambda a = 10$; (c) $a/b = 0.5$.

U_2 is proportional to $(\lambda a)^{-2}$ or the fluid permeability when λa is small and approaches a constant value when λa is large, whereas U_3 is not a sensitive function of λa and approaches constant values in both limits of λa . For specified values of κa and λa , U_2 and U_3 are monotonic decreasing functions of a/b (U_3 equals unity at $a/b = 0$ and vanishes at $a/b = 1$). When the electric double layers are thick (κa is small) or the fluid flow penetration inside the particle is thin (λa is large), the boundary effect on the electrokinetic mobility of the particle (the effect of a/b on U_2 and U_3) becomes significant.

The normalized electrokinetic migration velocity $\eta \kappa^2 U / Q E_\infty$ ($= U_2 + U_3 \kappa \sigma_b / Q$) of a charged porous sphere in a charged cavity calculated using eq 33 is plotted versus the dimensionless cavity-to-particle fixed charge density ratio $\kappa \sigma_b / Q$ in Figure 7 for various values of the parameters κa , λa , and a/b . Analogous to the case of a charged rigid sphere discussed in section 3.1,

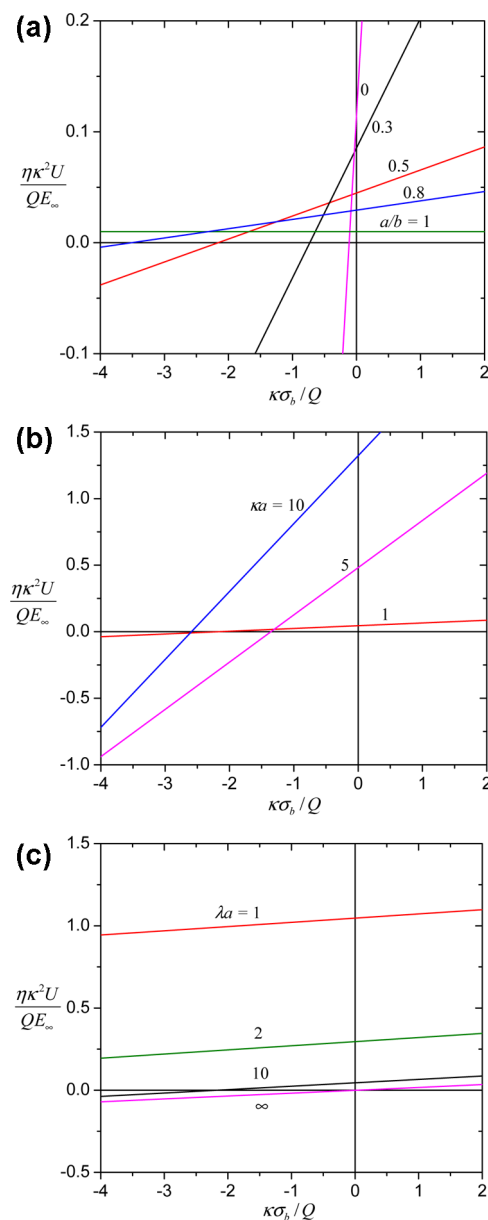


Figure 7. Plots of the normalized electrokinetic migration velocity $\eta \kappa^2 U / Q E_\infty$ for a charged porous sphere in a charged spherical cavity as calculated from eq 33 versus the dimensionless charge density ratio $\kappa \sigma_b / Q$: (a) $\kappa a = 1$ and $\lambda a = 10$; (b) $\lambda a = 10$ and $a/b = 0.5$; (c) $\kappa a = 1$ and $a/b = 0.5$.

the effect of the cavity wall will enhance/reduce the electrophoretic velocity of the porous particle if their fixed charge densities are of the same/opposite signs. The effect of the surface charge at the cavity wall on the particle migration can be significant as the magnitude of $\kappa \sigma_b / Q$ is large, and the particle may reverse the direction of its migration velocity when the value of $\kappa \sigma_b / Q$ decreases to less than about -1 . Again, the magnitude of $\eta \kappa^2 U / Q E_\infty$ in general increases with an increase in κa , decreases with an increase in λa , and decreases with an increase in a/b .

3.3. Electrokinetic Migration of a Soft Sphere in a Cavity. When a soft sphere undergoes electrophoresis in an unbounded electrolyte solution ($a/b = 0$), the term $U_3 \kappa \sigma_b$ in eq 33 disappears, and the mobility parameters U_1 and U_2 calculated from eq 34 are functions of the electrokinetic radius

κa , shielding parameter λa , and radius ratio r_0/a of the particle. The simplified formulas and numerical results of these functions are available in the literature,^{25,48} which indicate that a soft particle bearing no net charge [$r_0^2\sigma + (a^3 - r_0^3)Q/3 = 0$] can undergo electrophoresis and the direction of its electrophoretic velocity is decided by the sign of the fixed charges in the porous surface layer (Q) of the particle.

The mobility parameters U_1 , U_2 , and U_3 for a soft sphere in a spherical cavity calculated from eq 34 using the Dirichlet boundary condition in eq 13 for the applied electric potential at the cavity wall are plotted for various values of the parameters κa , λa , r_0/a , and a/b in Figures 8–10. Again, these mobility

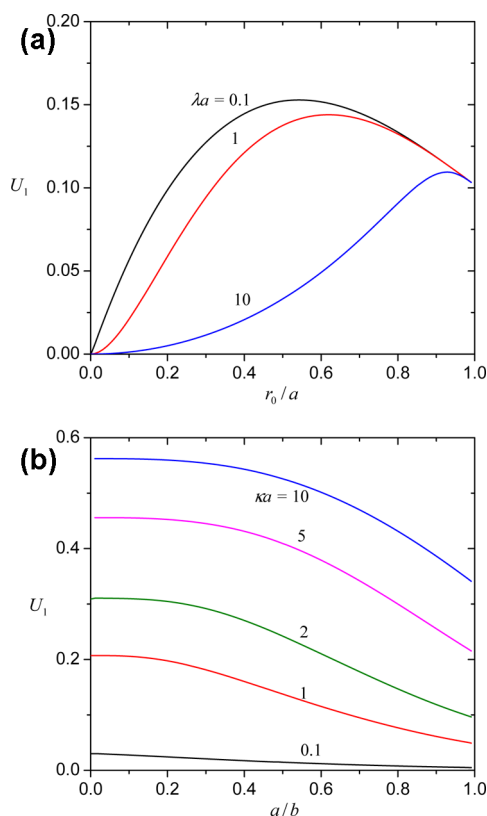


Figure 8. Plots of the mobility parameter U_1 for a charged soft sphere in a spherical cavity as calculated from eq 34: (a) $\kappa a = 1$ and $a/b = 0.5$; (b) $\lambda a = 1$ and $r_0/a = 0.5$.

parameters are always positive, in general decrease with an increase in a/b , increase with an increase in κa , and decrease with an increase in λa , analogous to the results for the limiting cases of $r_0/a = 1$ (in which λa is trivial) and $r_0/a = 0$ presented in sections 3.1 and 3.2. Similar results can be obtained if the Neumann boundary condition in eq 14 is used to replace the Dirichlet condition.

Figure 8a shows that the mobility parameter U_1 , which represents the contribution to the electrophoretic velocity of the confined soft particle from the surface charge density σ of its impermeable core, increases with an increase in r_0/a from zero at $r_0/a = 0$ (due to the increase in the effective surface charge of the impermeable core), reaches a maximum at some value of r_0/a , and then decreases with a further increase in r_0/a (due to the enhancement in hydrodynamic resistance to the particle migration caused by the increase in the volume ratio of the impermeable core in the particle) for given values of κa , λa , and a/b . Conversely, as shown in Figure 9a, the mobility

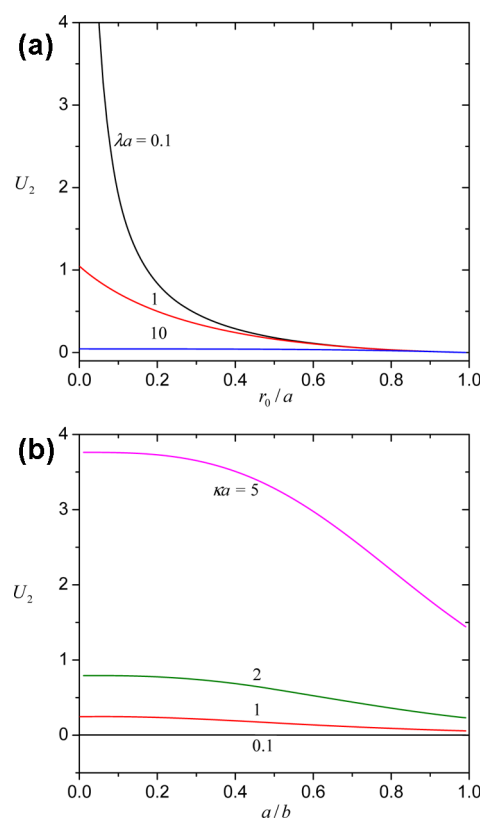


Figure 9. Plots of the mobility parameter U_2 for a charged soft sphere in a spherical cavity as calculated from eq 34: (a) $\kappa a = 1$ and $a/b = 0.5$; (b) $\lambda a = 1$ and $r_0/a = 0.5$.

parameter U_2 , which denotes the contribution to the electrophoretic velocity of the soft particle from the fixed charge density Q of its porous surface layer, decreases monotonically with an increase in r_0/a and vanishes when $r_0/a = 1$. In the case of moderate values of r_0/a (such as $r_0/a = 0.5$), the fixed charge densities σ and Q contribute comparably to the electrophoretic velocity of the soft sphere.

Figure 10a illustrates that the mobility parameter U_3 , which represents the contribution to the migration velocity of the soft particle from the surface charge density σ_b of its confining cavity wall, in general increases with an increase in r_0/a from a finite value at $r_0/a = 0$, reaches a maximum, and then decreases with a further increase in r_0/a to another finite value at $r_0/a = 1$. For specified values of the parameters κa , λa , r_0/a , a/b , σ_b/σ , and $+\kappa\sigma_b/Q$, the normalized electrokinetic migration velocity $\eta\kappa U/\sigma E_\infty$ or $\eta\kappa^2 U/QE_\infty$ of a charged soft sphere in a charged cavity can be readily calculated via eq 33 using the mobility parameters U_1 , U_2 , and U_3 .

The dielectric constant of the porous surface layer of the soft sphere has been assumed to equal that of the electrolyte solution. In fact, the effective permittivity $\alpha\epsilon$ in the region $r_0 \leq r < a$ should differ from (most likely, be smaller than) the fluid permittivity ϵ by a factor α . According to eqs 2 and 3, taking this effect into account is equivalent to replacing the fixed charge densities σ and Q of the soft particle by σ/α and Q/α , respectively, and the Debye parameter κ by $\kappa[1 - h(r)(1 - \alpha)]^{1/2}$ in the same formulation. Approximately, if $\alpha < 1$ ($\alpha > 1$), the electrophoretic mobility of the soft particle (predicted by eq 33) in an unbounded fluid will be increased (decreased) by a factor α and that in a spherical cavity can be increased or decreased depending on $\alpha\sigma_b/\sigma$, $\alpha\kappa\sigma_b/Q$, and other parameters.

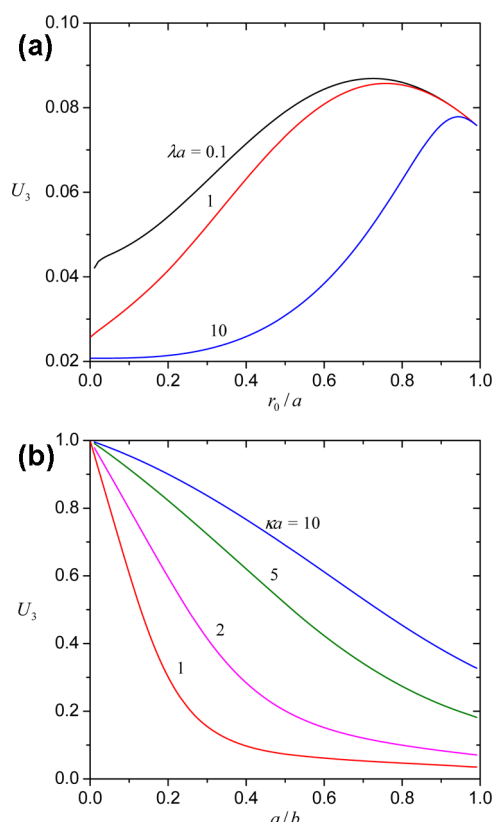


Figure 10. Plots of the mobility parameter U_3 for a soft sphere in a charged spherical cavity as calculated from eq 34: (a) $\kappa a = 1$ and $a/b = 0.5$; (b) $\lambda a = 1$ and $r_0/a = 0.5$.

4. CONCLUDING REMARKS

The quasi-steady electrophoretic motion of a charged soft sphere situated at the center of a charged spherical cavity filled with an arbitrary electrolyte solution is analyzed in this article. The porous shell of the soft particle is treated as a solvent-permeable and ion-penetrable layer of arbitrary thickness in which fixed-charged groups and frictional segments are distributed at uniform densities. The thickness of the electric double layers around the particle and adjacent to the cavity wall can be arbitrary relative to the particle radius.

The linearized Poisson–Boltzmann equation and the Laplace equation are solved for the equilibrium double-layer potential distribution and its perturbation caused by the applied electric field, respectively, for the fluid phase between the rigid core of the particle and the cavity wall. The modified Stokes and Brinkman equations governing the fluid flow fields outside and inside the porous surface layer of the particle, respectively, are solved subsequently. The requirement that the total force exerted on the soft particle is zero leads to eq 33 for its electrokinetic migration velocity in terms of the fixed charge densities on the rigid core surface, in the porous shell, and on the cavity wall, with the relevant mobility parameters U_1 , U_2 , and U_3 (functions of the electrokinetic radius κa , shielding parameter λa , and radius ratio r_0/a of the particle and the particle-to-cavity radius ratio a/b) given by eq 34.

The effect of the surface charge at the cavity wall on the migration of the particle can be significant as the magnitude of the dimensionless cavity-to-particle fixed charge density ratio is large, and the particle may reverse the direction of its velocity from that of electrophoresis in an unbounded fluid. Equation

33 for the migration velocity of a charged soft sphere in a concentric spherical cavity reduces to the corresponding formulas for a charged impermeable sphere and a charged porous sphere, respectively, in the limiting cases of $r_0/a = 1$ and $r_0/a = 0$.

Equations 6–10 are obtained on the basis of the Debye–Hückel approximation for the equilibrium potential distribution around a soft sphere in a cavity. A formula for the electrophoretic mobility of an impermeable sphere with low ζ potential in an unbounded fluid obtained by Henry¹ similar to eq 36a can be found to give good approximations for the case of a reasonably high ζ potential (with an error of about 5% in aqueous KCl solutions for the case of $|\zeta|e/kT = 2$, where e is the charge of a proton, k is Boltzmann's constant, and T is the absolute temperature).² Therefore, our results might be used tentatively for the situation of reasonably high fixed charge densities, say, $|\sigma|$ and $|Q|$ up to $ekT(\kappa a + 1)/2\pi a\epsilon$ and $ekT\kappa^2/e$ (or 10^{-3} C/m² and 10^5 C/m³), respectively.

AUTHOR INFORMATION

Corresponding Author

*Tel.: +886-2-33663048. Fax: +886-2-23623040. E-mail: huan@ntu.edu.tw.

Notes

The authors declare no competing financial interest.

ACKNOWLEDGMENTS

This research was supported by the National Science Council of the Republic of China.

REFERENCES

- (1) Henry, D. C. The Cataphoresis of Suspended Particles. Part I. The Equation of Cataphoresis. *Proc. R. Soc. London, Ser. A* **1931**, 133, 106–129.
- (2) O'Brien, R. W.; White, L. R. Electrophoretic Mobility of a Spherical Colloidal Particle. *J. Chem. Soc., Faraday Trans. 2* **1978**, 74, 1607–1626.
- (3) Jorgenson, J. W. Electrophoresis. *Anal. Chem.* **1986**, 58, 743A–760A.
- (4) Ewing, A. G.; Wallingford, R. A.; Olefirowicz, T. M. Capillary Electrophoresis. *Anal. Chem.* **1989**, 61, 292A–303A.
- (5) Keh, H. J.; Anderson, J. L. Boundary Effects on Electrophoretic Motion of Colloidal Spheres. *J. Fluid Mech.* **1985**, 153, 417–439.
- (6) Keh, H. J.; Chen, S. B. Electrophoresis of a Colloidal Sphere Parallel to a Dielectric Plane. *J. Fluid Mech.* **1988**, 194, 377–390.
- (7) Loewenberg, M.; Davis, R. H. Near-Contact Electrophoretic Particle Motion. *J. Fluid Mech.* **1995**, 288, 103–122.
- (8) Keh, H. J.; Chiou, J. Y. Electrophoresis of a Colloidal Sphere in a Circular Cylindrical Pore. *AIChE J.* **1996**, 42, 1397–1406.
- (9) Yariv, E.; Brenner, H. Near-Contact Electrophoretic Motion of a Sphere Parallel to a Planar Wall. *J. Fluid Mech.* **2003**, 484, 85–111.
- (10) Chang, Y. C.; Keh, H. J. Diffusiophoresis and Electrophoresis of a Charged Sphere Perpendicular to One or Two Plane Walls. *J. Colloid Interface Sci.* **2008**, 322, 634–653.
- (11) Zydney, A. L. Boundary Effects on the Electrophoretic Motion of a Charged Particle in a Spherical Cavity. *J. Colloid Interface Sci.* **1995**, 169, 476–485.
- (12) Lee, E.; Chu, J.-W.; Hsu, J.-P. Electrophoretic Mobility of a Sphere in a Spherical Cavity. *J. Colloid Interface Sci.* **1998**, 205, 65–76.
- (13) Keh, H. J.; Hsieh, T. H. Electrophoresis of a Colloidal Sphere in a Spherical Cavity with Arbitrary Zeta Potential Distributions and Arbitrary Double-Layer Thickness. *Langmuir* **2008**, 24, 390–398.
- (14) Lee, S. Y.; Yalcin, S. E.; Joo, S. W.; Sharma, A.; Baysal, O.; Qian, S. The Effect of Axial Concentration Gradient on Electrophoretic

Motion of a Charged Spherical Particle in a Nanopore. *Microgravity Sci. Technol.* **2010**, *22*, 329–338.

(15) Napper, D. H. *Polymeric Stabilization of Colloidal Dispersions*; Academic Press: London, 1983.

(16) Anderson, J. L.; Solomentsev, Y. Hydrodynamic Effects of Surface Layer on Colloidal Particles. *Chem. Eng. Commun.* **1996**, *148–150*, 291–314.

(17) Wunderlich, R. W. The Effects of Surface Structure on the Electrophoretic Mobilities of Large Particles. *J. Colloid Interface Sci.* **1982**, *88*, 385–397.

(18) Masliyah, J. H.; Neale, G.; Malysa, K.; van de Ven, T. G. M. Creeping Flow over a Composite Sphere: Solid Core with Porous Shell. *Chem. Eng. Sci.* **1987**, *42*, 245–253.

(19) Hill, R. J.; Saville, D. A.; Russel, W. B. Electrophoresis of Spherical Polymer-Coated Colloidal Particles. *J. Colloid Interface Sci.* **2003**, *258*, 56–74.

(20) Lopez-Garcia, J. J.; Grosse, C.; Horno, J. Numerical Study of Colloidal Suspensions of Soft Spherical Particles Using the Network Method. I. DC Electrophoretic Mobility. *J. Colloid Interface Sci.* **2003**, *265*, 327–340.

(21) Zhang, X.; Hsu, W.-L.; Hsu, J.-P.; Tseng, S. Diffusiophoresis of a Soft Spherical Particle in a Spherical Cavity. *J. Phys. Chem. B* **2009**, *113*, 8646–8656.

(22) Ahualli, S.; Jimenez, M. L.; Carrique, F.; Delgado, A. V. AC Electrokinetics of Concentrated Suspensions of Soft Particles. *Langmuir* **2009**, *25*, 1986–1997.

(23) Huang, P. Y.; Keh, H. J. Diffusiophoresis of a Spherical Soft Particle in Electrolyte Gradients. *J. Phys. Chem. B* **2012**, *116*, 7575–7589.

(24) Keh, H. J.; Liu, Y. C. Sedimentation Velocity and Potential in a Dilute Suspension of Charged Composite Spheres. *J. Colloid Interface Sci.* **1997**, *195*, 169–191.

(25) Liu, Y. C.; Keh, H. J. Electric Conductivity of a Dilute Suspension of Charged Composite Spheres. *Langmuir* **1998**, *14*, 1560–1574.

(26) Ohshima, H. Electrophoretic Mobility of Soft Particles in Concentrated Suspensions. *J. Colloid Interface Sci.* **2000**, *225*, 233–242.

(27) Duval, J. F. L.; Ohshima, H. Electrophoresis of Diffuse Soft Particles. *Langmuir* **2006**, *22*, 3533–3546.

(28) Dukhin, S. S.; Zimmermann, R.; Werner, C. Electrophoresis of Soft Particles at High Electrolyte Concentrations: An Interpretation by the Henry Theory. *J. Colloid Interface Sci.* **2007**, *313*, 676–679.

(29) Zhang, X.; Hsu, J.-P.; Chen, Z.-S.; Yeh, L.-H.; Ku, M.-H.; Tseng, S. Electrophoresis of a Charge-Regulated Soft Sphere in a Charged Cylindrical Pore. *J. Phys. Chem. B* **2010**, *114*, 1621–1631.

(30) Crawford, G. P. A Bright New Page in Portable Displays. *IEEE Spectrum* **2000**, *37* (10), 40–46.

(31) Crowley, J. M.; Sheridan, N. K.; Romano, L. Dipole Moments of Gyron Balls. *J. Electrostat.* **2002**, *55*, 247–259.

(32) Kawahata, S.; Ohshima, H.; Muramatsu, N.; Kondo, T. Charge Distribution in the Surface Region of Human Erythrocytes as Estimated from Electrophoretic Mobility Data. *J. Colloid Interface Sci.* **1990**, *138*, 182–186.

(33) Morita, K.; Muramatsu, N.; Ohshima, H.; Kondo, T. Electrophoretic Behavior of Rat Lymphocyte Subpopulations. *J. Colloid Interface Sci.* **1991**, *147*, 457–461.

(34) Makino, K.; Yamamoto, S.; Fujimoto, K.; Kawaguchi, H.; Ohshima, H. Surface Structure of Latex Particles Covered with Temperature-Sensitive Hydrogel Layers. *J. Colloid Interface Sci.* **1994**, *166*, 251–258.

(35) Blaakmeer, J.; Bohmer, M. R.; Cohen Stuart, M. A.; Fleer, G. J. Adsorption of Weak Polyelectrolytes on Highly Charged Surfaces. Poly(acrylic acid) on Polystyrene Latex with Strong Cationic Groups. *Macromolecules* **1990**, *23*, 2301–2309.

(36) Zharkikh, N. I.; Shilov, V. N. Theory of Collective Electrophoresis of Spherical Particles in the Henry Approximation. *Colloid J. USSR (Engl. Transl.)* **1982**, *43*, 865–870.

(37) Dukhin, A. S.; Shilov, V.; Borkovskaya, Yu. Dynamic Electrophoretic Mobility in Concentrated Dispersed Systems. *Cell Model. Langmuir* **1999**, *15*, 3452–3457.

(38) Zholkovskij, E. K.; Masliyah, J. H.; Shilov, V. N.; Bhattacharjee, S. Electrokinetic Phenomena in Concentrated Disperse Systems: General Problem Formulation and Spherical Cell Approach. *Adv. Colloid Interface Sci.* **2007**, *134–135*, 279–321.

(39) Levine, S.; Neale, G. H. The Prediction of Electrokinetic Phenomena within Multiparticle Systems I. Electrophoresis and Electroosmosis. *J. Colloid Interface Sci.* **1974**, *47*, 520–529.

(40) Kozak, M. W.; Davis, E. J. Electrokinetics of Concentrated Suspensions and Porous Media. I. Thin Electrical Double Layers. *J. Colloid Interface Sci.* **1989**, *127*, 497–510.

(41) Matsumoto, K.; Suganuma, A. Settling Velocity of a Permeable Model Floc. *Chem. Eng. Sci.* **1977**, *32*, 445–447.

(42) Masliyah, J. H.; Polikar, M. Terminal Velocity of Porous Spheres. *Can. J. Chem. Eng.* **1980**, *58*, 299–302.

(43) Aoyanagi, O.; Muramatsu, N.; Ohshima, H.; Kondo, T. Electrophoretic Behavior of PolyA-Graft-PolyB-Type Microcapsules. *J. Colloid Interface Sci.* **1994**, *162*, 222–226.

(44) Chen, W. C. *Electrophoresis of a Charged Soft Particle in a Charged Cavity*. M.S. Thesis, National Taiwan University, Taipei, 2013.

(45) Ohshima, H. Electrophoretic Mobility of Soft Particles. *J. Colloid Interface Sci.* **1994**, *163*, 474–483.

(46) Liu, Y. C.; Keh, H. J. The Electric Conductivity of Dilute Suspensions of Charged Porous Spheres. *J. Colloid Interface Sci.* **1997**, *192*, 375–385.

(47) Wei, Y. K.; Keh, H. J. Diffusiophoretic Mobility of Charged Porous Spheres in Electrolyte Gradients. *J. Colloid Interface Sci.* **2004**, *269*, 240–250.

(48) Ding, J. M.; Keh, H. J. Electrophoretic Mobility and Electric Conductivity in Dilute Suspensions of Charge-Regulating Composite Spheres. *Langmuir* **2003**, *19*, 7226–7239.